Error Corrections for an Automated Time-Domain Network Analyzer

WAYMOND R. SCOTT, JR., MEMBER, IEEE, AND GLENN S. SMITH, FELLOW, IEEE

Abstract—**The errors are considered for an automated time-domain network analyzer based on a Tektronix sampling oscilloscope. Procedures are presented for removing the errors produced by two important sources: unwanted reflections associated with discontinuities and nonlinearities in the time base of the oscilloscope. The effectiveness of the error correction procedures is demonstrated by measurements of standard terminations with known reflection coefficients.**

I. Introduction

IN AN automated time-domain network analyzer, a repetitive impulsive waveform is incident on the device under test. The incident waveform and the waveform of the signal reflected from the device, or the waveform of the signal transmitted through the device, are measured with a sampling oscilloscope. These waveforms are digitized and passed to a processing computer where they are corrected for errors and Fourier transformed (FFT). The transformed waveforms are then used to compute the desired network parameters, such as the reflection or transmission coefficient, over a wide band of frequencies. Several automated time-domain network analyzers have been described in the literature [1]–[4], and the progress in the state of the technology in this area has been documented in a series of articles by N. Nahman of the National Bureau of Standards [5]–[7].

At the present time, the only commercially available sampling oscilloscope plug-ins are those available from Tektronix Inc. An automated time-domain measurement system is formed by placing these plug-ins in a Tektronix digital-processing oscilloscope mainframe, which is interfaced to a computer. The errors in this system are discussed in this paper. The error-correcting procedures presented, however, are general, and they can be used with any time-domain measurement system.

II. Measurement System

Fig. 1 is a block diagram of the measurement system configured to measure the reflection coefficient of the device under test. The time-domain waveforms are measured with a sampling oscilloscope which automatically digitizes and stores the waveforms as 512 uniformly spaced samples. The sampling oscilloscope consists of a Tektronix 7704A mainframe with a 7001 processing unit. A 7S12 sampling unit is used in the mainframe with a *S*-6 feedthrough sampling head and a *S*-53 trigger recognizer. The oscilloscope is interfaced to a computer that is used to store and process the waveforms. Each waveform is averaged 500 times to reduce the effects of noise; this takes about 2 min for each waveform.

An Avtech model AVH-S pulse generator produces the incident pulse. The shape of the pulse is not ideal for the measurement. A filter, a simple *RC* network, is used to shape the spectrum of the pulse so that it is more uniform over the usable frequency range (50 MHz–2 GHz). The pulse and its spectrum, before and after filtering, are shown in Fig. 2. Notice that the spectrum of the filtered pulse is more uniform over this frequency range (frequencies up to the dashed line in Fig. 2) than that of the unfiltered pulse.

The pulser is connected to the input of the feedthrough sampler by a 15-ns delay line, and the output of the feedthrough sampler is connected to a 30-cm GR-900 precision delay line (1 ns). The end of this line, *A-A'* in Fig. 1, is the reference plane for measuring the reflection coefficient of the device under test. The repetitive output of a second-pulse generator (Tektronix Model PG 501) is used to trigger the Avtech pulser and to trigger the sampling unit.

There are several identifiable sources of error in this time-domain measurement system. These can roughly be divided into errors associated with the instrumentation and errors associated with the signal processing. These errors are catalogued in Table I.

A major source of error in the instrumentation is the unwanted reflections that arise at discontinuities in the system, such as imperfect connections. Unwanted reflections can often be removed by using a delay line to place them out of the measurement time window. For example, in the system shown in Fig. 1, the 15-ns delay causes the multiple reflection between the feedthrough sampler and the 13-dB attenuator to appear 28 ns after the reflection from the reference plane *A-A'*. Not all of the unwanted reflections can be removed by introducing delay lines; this is particularly true of the reflections between the sampler

Manuscript received July 9, 1985; revised January 13, 1986. This work was supported in part by the Joint Services Electronics Program under Contracts DAAG29-81-K-0024 and DAAG29-84-K-0024, and by a Specialized Research Equipment Grant from the National Science Foundation, ENG77-17200.

The authors are with the School of Electrical Engineering, Georgia Institute of Technology, Atlanta, GA 30332. W. R. Scott was the recipient of the TRW Foundation Augmentation Fellowship during this research.

IEEE Log Number 8608780.

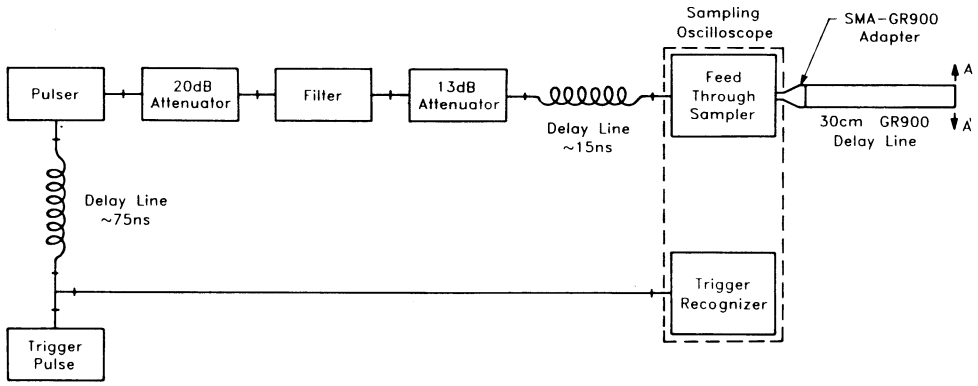

Fig. 1. Block diagram of the measurement system.

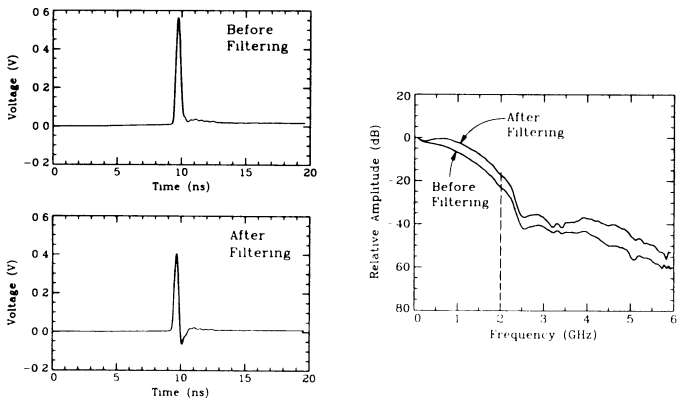

Fig. 2. The incident pulse and its spectrum, before and after filtering.

TABLE I
ERRORS IN THE TIME-DOMAIN MEASUREMENT SYSTEM

Instrumentation Errors	
Unwanted Reflections	- caused by discontinuities at connectors, etc.
Nonlinearities	- associated with the vertical and horizontal scales.
Drift	- long term changes in the time base.
Jitter	- short term uncertainties in the time base (trigger jitter).
Signal Processing Errors	
Truncation Error	- caused by the portion of the waveform outside the finite measurement window.
Aliasing	- a result of using a finite number of samples to represent a continuous waveform.

and the device under test. A method for removing these reflections will be presented in the next section.

The vertical and the horizontal scales (amplitude and time) of the sampling unit may exhibit nonlinearities as a result of nonlinearities in the vertical amplifier, timing ramp, etc. For the system tested, the nonlinearity in the vertical scale was insignificant; however, the nonlinearity in the horizontal scale (time base) was appreciable. This was corrected using the procedure described in the next section.

There is also an error in the measured waveform caused by the fluctuations in the time base. This error is divided into two classes. The first is the jitter which is the short-term random fluctuations in the time base, and the second is the drift which is the long-term systematic fluctuations in the time base. For an averaged waveform, the effect of stationary jitter (short-term random fluctuations in the time base that exhibit time-invariant statistics) is to low-pass filter the waveform [1]. This effect does not cause an error in the determination of the reflection coefficient. It is difficult, if not impossible, to remove the effects of the systematic drift that occurs while the oscilloscope is measuring a single waveform; however, the systematic drift that occurs between the measurement of two waveforms can be removed using a procedure presented in [4].

The errors introduced by the signal processing are primarily the result of windowing and sampling the continuous waveforms. These errors, such as truncation error and aliasing, are discussed in detail in the literature [8]. To prevent truncation error, the complete waveform, or a good approximation of it, must be contained in the measurement window. If the waveform includes a step-like component which has settled at both ends of the window, the waveform can be processed using algorithms proposed by A. M. Nicolson [9] and W. L. Gans and N. S. Nahman [1], [10]. Aliasing is controlled by keeping the rate at which the waveform is sampled significantly higher than the Nyquist rate [8].

III. Error Corrections

The removal of the unwanted reflections is considered first; this is performed in the frequency domain. A reduced model for the measurement system is shown in Fig. 3(a). In this model, the pulser, the input side of the feedthrough sampler, and all of the components between them are grouped together to form a "new pulser." The output side of the sampler, the adapter, and the GR-900 delay line are also grouped together to form a single two-port network. The signal flow graph for this model is shown in Fig. 3(b). In this graph, $V_p(j\omega)$ is the Fourier transform of the pulse generated by the "new pulser," and $\rho_p(j\omega)$ is the reflection coefficient looking into the "new pulser." The quantities $\rho_1(j\omega)$, $\rho_2(j\omega)$, $\tau_1(j\omega)$, and $\tau_2(j\omega)$ are the S-parameters of the two-port network. $V_m(j\omega)$ is the Fourier transform of the waveform measured by the feedthrough sampler, and $\rho_l(j\omega)$ is the reflection coefficient of the termination. The object of the

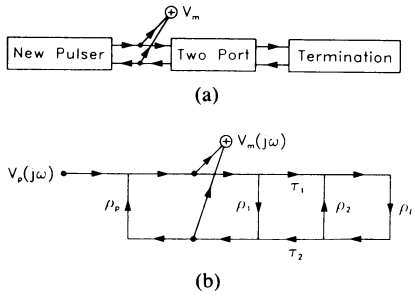

Fig. 3. (a) Reduced model for the measurement system. (b) Signal Flow Graph for the measurement system.

analysis is to develop a procedure for determining the reflection coefficient of a termination with the effects of the unwanted reflections removed.

The signal flow graph in Fig. 3(b) is solved to find V_m in terms of the other elements:

$$V_m = \left[1 + \frac{\rho_1(1 + \rho_p) + \rho_l(1 + \rho_p)(\tau_1\tau_2 - \rho_1\rho_2)}{(1 - \rho_p\rho_1)(1 - \rho_l\rho_s)}\right] V_p \tag{1}$$

where

$$\rho_s = \rho_2 - \frac{\rho_p\tau_1\tau_2}{1 - \rho_p\rho_1}. \tag{2}$$

Note that when the second term on the right-hand side of (2) is small, as it is in the present case, ρ_s is approximately the reflection coefficient looking into the GR-900 delay line toward the sampler. Now, consider the frequency-domain representation of the waveforms that are measured when the termination is:

(i) an unknown load, $\rho_l = \rho$, $V_m = V_{mu}$;
(ii) and ideal matched load, $\rho_l = 0$, $V_m = V_{mm}$;
(iii) an ideal short circuit, $\rho_l = -1$, $V_m = V_{ms}$;
(iv) an ideal open circuit offset by the length l_o, $\rho_l = \rho_o = \exp(-j\omega 2l_o/c)$ with $l_o \ll \lambda_o/4$, $V_m = V_{mo}$.

The quantity M is defined to be

$$M = \frac{V_m - V_{mm}}{V_{ms} - V_{mm}} = -\frac{\rho_l(1 + \rho_s)}{1 - \rho_l\rho_s}. \tag{3}$$

Let $M = M_u$ when the termination is an unknown load ($\rho_l = \rho$), and let $M = M_o$ when the termination is an open circuit ($\rho_l = \rho_o$). The reflection-coefficient ρ of the unknown load is then

$$\rho = -\frac{M_u}{1 - \rho_s(M_u - 1)} \tag{4}$$

where

$$\rho_s = \frac{M_o/\rho_o + 1}{M_o - 1}. \tag{5}$$

Thus the uncorrupted reflection coefficient ρ of the unknown load can be determined from V_{mu}, V_{mm}, V_{ms}, and V_{mo} by applying (3) to obtain M_u and M_o, then applying (5) to obtain ρ_s, and finally applying (4). Figure 4(a) is a graph of the magnitude of the reflection-coefficient ρ_s as a function of frequency. Note that four curves, each from a separate measurement, are shown in Fig. 4(a) to demonstrate the repeatability of the calibration.

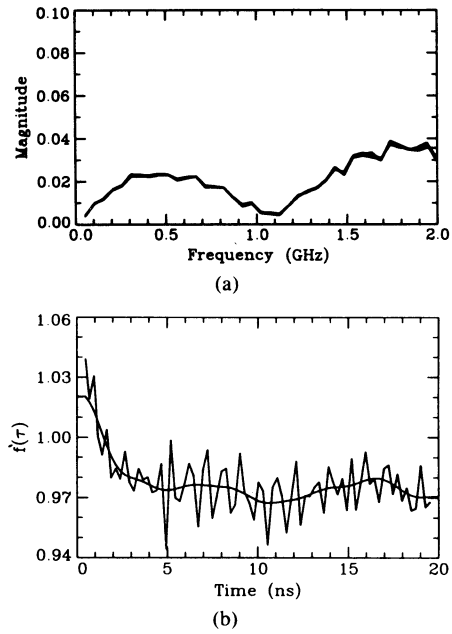

Fig. 4. (a) Graph of the magnitude of the reflection coefficient ρ_s as a function of frequency. (b) Typical time calibration curve, before and after smoothing.

Next, the removal of the errors produced by the nonlinearities in the time base of the oscilloscope will be considered. The sampling oscilloscope should sample the waveforms at equally spaced intervals in time, but it does not. The magnitude of this error decreases as the time delay between the trigger pulse for the sampling oscilloscope and the start of the measurement window increases. This error is removed by using a long time delay between the trigger pulse and the start of the measurement window and then by calibrating the time base to remove the remaining nonlinearity.

The nonlinearity in the time base is determined by measuring a sinusoidal waveform of known frequency. Let τ be the time measured by the sampling oscilloscope, and let t be the actual time. Assume that t is a function of τ, $t = f(\tau)$. The zero crossings of the waveform and the zero crossings of its first derivative are computed: τ_i, $i = 1, 2, 3, \cdots, m$. Now the first derivative of $f(\tau)$ at the discrete times $\bar{\tau}_i = (\tau_{i+1} + \tau_i)/2$ is approximately equal to the ratio between the actual time increment determined from the known frequency and the measured time increment determined from the zero crossings:

$$f'(\bar{\tau}_i) \approx \frac{\text{Actual Time Increment}}{\text{Measured Time Increment}} = \frac{T/4}{\tau_{i+1} - \tau_i}, \quad i = 1, 2, 3, \cdots, m - 1 \tag{6}$$

where T is the period of the sinusoidal waveform. The correction $f'(\tau)$ for other values of τ is formed by linearly interpolating between the closest known values. The correction f' computed in this manner is rather noisy; it can be smoothed since it varies much more slowly than the

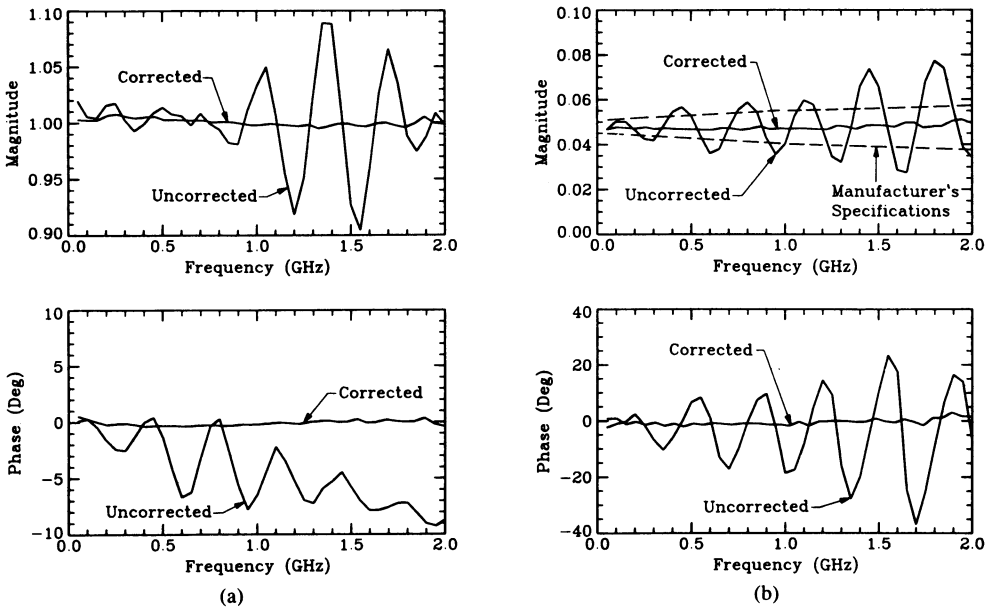

Fig. 5. Graphs of the uncorrected and corrected reflection coefficients. (a) The offset short-circuited termination. (b) The mismatched termination.

noise. Fig. 4(b) is a typical time calibration curve f' before and after smoothing. This curve was constructed using a sinusoidal waveform with a frequency of 1 ± 0.0001 GHz.

Now the function $f'(\tau)$ will be used to correct the time at each of the 512 sampled points of a measured waveform. The actual time at each of the sampled points is approximately

$$t_j \approx t_{j-1} + \Delta\tau f'(j\Delta\tau), \quad j = 1, 2, 3, \cdots, 511 \quad (7)$$

where $\Delta\tau$ is the measured time interval between the samples. For future processing, the points on the waveform need to be uniformly spaced in time. For each of the waveforms that is to be time corrected, a cubic spline is fit through the sampled points using the actual times t_i; then the spline is used to evaluate the waveform at uniformly spaced times.

Measurements were made of the reflection coefficients of standard GR-900 terminations to demonstrate the effectiveness of the above corrections. Results for two terminations, an offset short circuit ($|\rho| = 1.0$, offset = 7.521 cm) and a mismatched termination ($|\rho| = 0.045$) are shown in Fig. 5. These terminations represent two extremes: a large reflection coefficient and a small reflection coefficient. For each termination, the reflection coefficients (amplitude and phase) with all of the corrections applied and with none of the corrections applied are compared. In each of the graphs, the linear component of the phase due to the physical offset is removed. These graphs clearly indicate the need for the corrections and their effectiveness in increasing the accuracy of the measurements.

IV. Conclusions

An automated time-domain network analyzer was constructed. The system is based on a Tektronix sampling unit and digital-processing oscilloscope. The errors for the system, both instrumentation errors and signal-processing errors, were considered. Two important sources of error where identified: unwanted reflections associated with discontinuities, particularly at the feedthrough sampler, and nonlinearities in the time base of the oscilloscope. Procedures were developed for correcting the errors due to both sources. The effectiveness of these procedures was demonstrated by measurements of standard terminations with known reflection coefficients.

References

[1] W. L. Gans and J. R. Andrews, "Time domain automated network analyzer for measurement of RF and microwave components," National Bureau of Standards, Tech. Note 672, Sept. 1975.

[2] A. M. Nicolson, C. L. Bennett, D. Lamensdorf, and L. Susman, "Application of time-domain metrology to the automation of broadband microwave measurements," *IEEE Trans. Microwave Theory Tech.*, vol. MTT-20, pp. 3-9, Jan. 1972.

[3] P. R. Rigg and J. E. Carroll, "Low-cost computer-based time-domain microwave network analyser," *IEEE Proc.*, vol. 127, pt. H, pp. 107-111, Apr. 1980.

[4] J. Peyrelasse, C. Boned, and J. P. LePetite, "Setting up of a time domain spectroscopy experiment. Application to the study of the dielectric relaxation of pentanol isomers," *J. Phys. E: Sci. Instrum.*, vol. 14, pp. 1002-1008, 1981.

[5] N. S. Nahman, "The measurement of baseband-pulse risetimes of less than 10^{-9} S," *Proc. IEEE*, vol. 55, pp. 855-864, June 1967.

[6] ——, "Picosecond-domain waveform measurements," *Proc. IEEE*, vol. 66, pp. 441-454, Apr. 1978.

[7] ——, "Picosecond-domain waveform measurement: Status and future directions," *IEEE Trans. Instrum. Meas.*, vol. IM-32, pp. 117-124, Mar. 1983.

[8] E. O. Brigham, *The Fast Fourier Transform.* New York: Prentice-Hall, 1974.

[9] A. M. Nicolson, "Forming the fast-Fourier transform of a step response in time-domain metrology," *Electron. Lett.*, vol. 9, pp. 317-318, July 12, 1973.

[10] W. L. Gans and N. S. Nahman, "Continuous and discrete Fourier transforms of steplike waveforms," *IEEE Trans. Instrum. Meas.*, vol. IM-31, pp. 97-101, June 1982.